

Algebraic spiral solutions of the 2d incompressible Euler equations

Volker Elling

Abstract. We construct a class of self-similar 2d incompressible Euler solutions that have initial vorticity of mixed sign. The regions of positive and negative vorticity form algebraic spirals.

Keywords: incompressible Euler, vortex, vorticity, spiral, uniqueness.

Mathematical subject classification: 76B47, 76B03.

1 Main result

Theorem 1 ([11]). *Consider the 2d incompressible Euler equations*

$$\mathbf{v}_t + \nabla \cdot (\mathbf{v} \otimes \mathbf{v}) + \nabla \omega = 0, \quad (1)$$

$$\nabla \cdot \mathbf{v} = 0 \quad \text{on } \mathbb{R}^2 \times]0, \infty[\quad (2)$$

with self-similar initial data (see Fig. 1 left)

$$\omega(\mathbf{x}, t) \stackrel{r \searrow 0}{\rightarrow} r^{-\frac{1}{\mu}} \hat{\omega}(\theta), \quad (3)$$

where $\omega = \nabla \times \mathbf{v}$ is vorticity and (r, θ) are polar coordinates centered in $\mathbf{x} = 0$. Given $\epsilon > 0$ and $\mu \in]\frac{2}{3}, \infty[$, there is an $N_0 \in \mathbb{N}$ so that a weak solution of (1) and (3) exists for all initial data $\hat{\omega}$ satisfying the following conditions:

1. *Sufficiently high symmetry:* $\hat{\omega}$ is $\frac{2\pi}{N}$ -periodic for $N \geq N_0$.
2. *Dominant sign:* the Fourier coefficients satisfy

$$|\hat{\omega}^\wedge(0)| \geq \epsilon \sum_{n \neq 0} |\hat{\omega}^\wedge(n)|. \quad (4)$$

There are two choices of data: μ , which determines the radial asymptotics of initial vorticity, and $\hat{\omega}$, which is the angular distribution of vorticity on the unit circle (circle in Fig. 1 left). If the initial data is sufficiently symmetric, we can solve the problem for “large” initial data, allowing for regions of zero vorticity (a necessary prerequisite for studying evolution of vortex patches with non-regular boundary [1, 3, 4]) and in particular for flows with a mix of positive and negative vorticity (Fig. 1 left). In such initial data, vorticity of each sign would be in open cones with apex in the origin (Fig. 1 left).

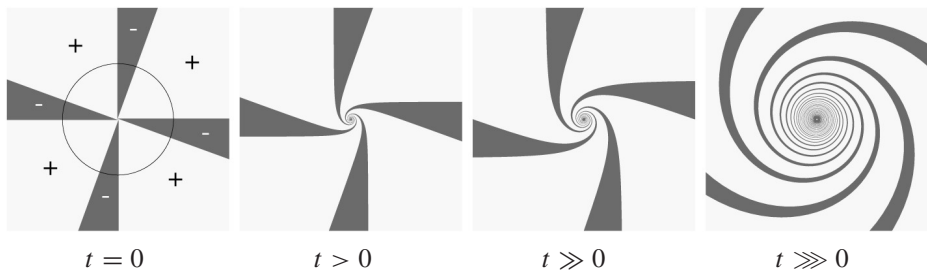


Figure 1: Left: initial vorticity with mixed sign; center: rollup into algebraic spirals; right: the spirals grow in time.

If $\hat{\omega}^\wedge(0) \neq 0$, then there is a net rotation around the origin, so intuition suggests the cone tips will curl up into spirals (Fig. 1 center), although their nature (e.g. algebraic or logarithmic) is not obvious a priori. Indeed [11] proves:

Remark 1. In the solutions of Theorem 1, for any $t > 0$ the boundaries between the regions of positive, zero and negative ω are algebraic spirals, parametrized by

$$\mathbf{x}(\theta) = f(\theta)\theta^{-\mu} \begin{bmatrix} \cos \theta \\ \sin \theta \end{bmatrix}, \quad 0 < \inf f \leq \sup f < \infty. \quad (5)$$

Flows with spiral rollup are important in applications since they are ubiquitous in physics [28], in trailing vortices at aircraft wings, flow past a sharp corner, Mach reflections [2], turbulent eddies, detaching boundary layers, the Moore singularity of vortex sheets [24], etc. But prior to our work the mathematically rigorous construction of algebraic spiral flows was unsuccessful; see [12, 19, 23] for various attempts and insights. Even numerical approximation is notoriously difficult and unstable [13, 20, 21, 22].

Since our initial data is self-similar, one would expect self-similar solutions as well, and indeed [11] show:

Remark 2. The solutions of Theorem 1 have the form

$$\omega(\mathbf{x}, t) = t^{-1} \underbrace{\omega(\underbrace{t^{-\mu} \mathbf{x}}_{=\check{\mathbf{x}}}, 1)}_{=\check{\omega}(\check{\mathbf{x}})} \quad , \quad \mathbf{v}(\mathbf{x}, t) = t^{\mu-1} \underbrace{\mathbf{v}(t^{-\mu} \mathbf{x}, 1)}_{=\check{\mathbf{v}}} \quad ,$$

$$\psi(\mathbf{x}, t) = t^{2\mu-1} \underbrace{\psi(t^{-\mu} \mathbf{x}, 1)}_{=\check{\psi}} \quad .$$
(6)

Hence the solution looks the same at all times $t > 0$ except dilated (by a factor t^μ) and scaled; $t \searrow 0$ is like zooming into the origin while $t \nearrow \infty$ is zooming away. To understand the t exponents, observe that $\omega = \nabla \times \mathbf{v}$ has dimensions of inverse time so that the initial condition (3) relates length to time to the power μ . The quantities $\check{\mathbf{x}}, \check{\psi}, \check{\mathbf{v}}, \check{\omega}$ are *dimensionless*.

Finally, we control the asymptotic behaviour of the solutions:

Remark 3. The solutions of Theorem 1 satisfy

$$\mathbf{v} = O(r^{1-\frac{1}{\mu}}) \quad \text{and} \quad \omega = O(r^{-\frac{1}{\mu}})$$

as $r \searrow 0$ and as $r \nearrow \infty$, uniformly in $t \in [0, \infty]$;

(7)

\mathbf{v}, ω are continuous in $\mathbf{x} \neq 0$.

The symmetry and dominant-sign assumptions will be relaxed in future work, but cannot be expected to be fully removable, as simple arguments show. Consider for example $\mu = 1$ and $\check{\omega} = \mathbf{1}_{[0, \pi]}$ so that $\omega(y_1, y_2) = \mathbf{1}_{]0, \infty[}(y_2)$, then the Biot-Savart integral

$$\int_{\mathbb{R}^2} \frac{(\mathbf{x} - \mathbf{y})^\perp}{|\mathbf{x} - \mathbf{y}|^2} \omega(\mathbf{y}) d\mathbf{y}$$

is undefined in every $\mathbf{x} \in \mathbb{R}^2$. Moreover, when (4) is not imposed, then dominance can change from positive to negative vorticity, causing the spiral to flip from counterclockwise to clockwise, with non-spiral borderline cases expected. Finally, the numerical work of Pullin [21, 22] on self-similar vortex sheet shows complicated bifurcation phenomena with limit points and non-uniqueness (which is our main motivation [9]), a field of major recent activity ([7, 8, 14, 16, 17, 25, 26, 27], see also [29, 30, 31]).

Standard theorems [5, 6, 15, 18] cannot recover the existence results of Theorem 1 because they either require much more regular initial data and/or assume single-signed initial vorticity.

2 Coordinate changes

Before we demonstrate how algebraic vortex spirals arise and what obstacles are overcome, it is convenient to perform several changes of coordinates. We make use of

$$f = \nabla_{\mathbf{x}} \cdot \mathbf{w} \iff f \det \mathbf{x}_y = \nabla_y \cdot (\text{adj } \mathbf{x}_y \mathbf{w}) \quad (8)$$

The divergence constraint (2) $\nabla_{\mathbf{x}} \cdot \mathbf{v} = 0$ is equivalent to

$$\mathbf{v} = \nabla_{\mathbf{x}}^{\perp} \psi \quad (9)$$

for a scalar *stream function* ψ . Taking the curl of the Euler equations (1) yields the *vorticity formulation*

$$0 = \partial_t \omega + \mathbf{v} \cdot \nabla_{\mathbf{x}} \omega \quad (10)$$

(6) reduces the problem to

$$0 = \check{\mathbf{q}} \cdot \nabla_{\check{\mathbf{x}}} \check{\omega} - \check{\omega} \quad , \quad \check{\mathbf{v}} = \nabla_{\check{\mathbf{x}}}^{\perp} \check{\psi} \quad , \quad \check{\omega} = \Delta_{\check{\mathbf{x}}} \check{\psi}$$

where

$$\check{\mathbf{q}} = \check{\mathbf{v}} - \mu \check{\mathbf{x}} \quad (11)$$

is the *pseudo-velocity*. Solutions of transport equations are more regular along integral curves of the transport vector $\check{\mathbf{q}}$, here called *pseudo-streamlines*; $\check{\omega}$ has constant sign on each of them, so they separate regions of positive, zero and negative vorticity.

To study spirals converging to a common origin, it is convenient to make a (conformal) change to *log-polar* coordinates

$$\mathbf{a} = (\ell, \theta) \quad , \quad \ell = \log \check{r} \quad , \quad \check{r} = |\check{\mathbf{x}}| \quad , \quad \theta = \angle \check{\mathbf{x}}$$

(see Fig. 2).

Nonlinear transport equations are awkward because the transport vector changes with the solution. We map pseudo-streamlines to lines by further changing to coordinates $\mathbf{b} = (\beta, \phi)$ where $\partial_{\beta} \parallel \check{\mathbf{q}}$ (see Fig. 3). We calculate the consequences first, before defining \mathbf{b} completely later:

$$\begin{aligned} \check{\mathbf{q}}^{\check{\mathbf{x}}} \cdot \nabla_{\check{\mathbf{x}}} &= (\nabla_{\check{\mathbf{x}}} \check{\psi}^{\perp} - \mu \check{\mathbf{x}}) \cdot \nabla_{\check{\mathbf{x}}} \\ &= (\nabla_{\check{\mathbf{x}}} \check{\psi} + \mu \check{\mathbf{x}}^{\perp}) \times \nabla_{\check{\mathbf{x}}} \\ &= \det \nabla_{\check{\mathbf{x}}} \mathbf{b}^T (\nabla_{\mathbf{b}} \check{\psi} + \mu \nabla_{\mathbf{b}} \check{\mathbf{x}}^T \check{\mathbf{x}}^{\perp}) \times \nabla_{\mathbf{b}} \\ &= \frac{1}{\check{\mathbf{x}}_{\beta} \times \check{\mathbf{x}}_{\phi}} ((\check{\psi}_{\beta} + \mu \check{\mathbf{x}} \times \check{\mathbf{x}}_{\beta}) \partial_{\phi} - (\check{\psi}_{\phi} + \mu \check{\mathbf{x}} \times \check{\mathbf{x}}_{\phi}) \partial_{\beta}) \end{aligned} \quad (12)$$

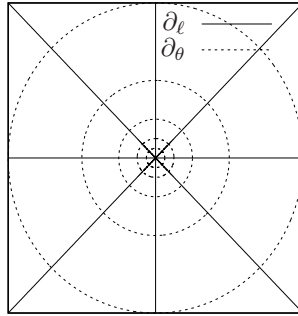


Figure 2: $\mathbf{a} = (\ell, \theta)$ log-polar coordinates.

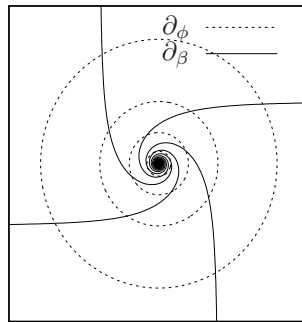


Figure 3: $\mathbf{b} = (\beta, \phi)$ coordinates (for $\check{\psi}_0$). Fixing ϕ picks the pseudo-streamline (solid curve) with angle ϕ at infinity; β is the angle travelled along it around the center, with $\beta = 0$ at spatial infinity while $\beta \rightarrow \infty$ is approaching the center.

We want the coefficient of ∂_ϕ to vanish, so if $\check{\mathbf{x}}_\beta \times \check{\mathbf{x}}_\phi \neq 0$ (else the transform is degenerate), then

$$0 = \check{\psi}_\beta + \mu \check{\mathbf{x}} \times \check{\mathbf{x}}_\beta \quad . \tag{13}$$

Assume this holds. Then taking ∂_ϕ yields

$$\begin{aligned} 0 &= \check{\psi}_{\beta\phi} + \mu(\check{\mathbf{x}} \times \check{\mathbf{x}}_\beta)_\phi \\ &= \check{\psi}_{\beta\phi} + \mu(\check{\mathbf{x}}_\phi \times \check{\mathbf{x}}_\beta + \check{\mathbf{x}} \times \check{\mathbf{x}}_{\beta\phi}) \\ &= \check{\psi}_{\beta\phi} + \mu(-2\check{\mathbf{x}}_\beta \times \check{\mathbf{x}}_\phi + (\check{\mathbf{x}} \times \check{\mathbf{x}}_\phi)_\beta) \\ &\Leftrightarrow \frac{1}{2\mu}(\check{\psi}_\phi + \mu \check{\mathbf{x}} \times \check{\mathbf{x}}_\phi)_\beta = \check{\mathbf{x}}_\beta \times \check{\mathbf{x}}_\phi = \det \nabla_{\mathbf{b}}^T \check{\mathbf{x}} \quad . \end{aligned} \tag{14}$$

Substituting this and (13) into (12) yields

$$\check{\mathbf{q}} \cdot \nabla_{\check{\mathbf{x}}} = -2\mu \underbrace{\frac{1}{\partial_\beta \log(\check{\psi}_\phi + \mu \check{\mathbf{x}} \times \check{\mathbf{x}}_\phi)}}_{=: \check{q}^\beta} \partial_\beta . \tag{15}$$

With this, the vorticity equation (2) reduces to

$$0 = \check{q}^\beta \partial_\beta \check{\omega} - \check{\omega} \tag{16}$$

which yields the surprisingly elegant solution

$$\check{\omega} = (\check{\psi}_\phi + \mu \check{\mathbf{x}} \times \check{\mathbf{x}}_\phi)^{-\frac{1}{2\mu}} \Omega(\phi) \tag{17}$$

where Ω is an integration constant. The appearance of Ω is natural: we have a choice of initial data that is also self-similar, hence constant along rays, which are constant- ϕ contours. (Ω does not correspond exactly to $\dot{\omega}$.)

The scalar constraint (13) fixes only “one half” of the coordinate transform. To fix the other half, it is natural (given the spiral behaviour) to make β and ϕ angles (Fig. 3):

$$\theta = \beta + \phi \tag{18}$$

where $\mathbf{a} = (\ell, \theta)$ are $\check{\mathbf{x}}$ log-polar coordinates (Fig. 2).

Using (for any homogeneous first-order operator ∂) $\check{\mathbf{x}} \times \partial \check{\mathbf{x}} = \check{r}^2 \partial \theta = e^{2\ell} \partial \theta$, we solve the constraint (13) for

$$\ell = \frac{1}{2} \log \frac{\check{\psi}_\beta}{-\mu} . \tag{19}$$

The *solution-dependent* change of coordinates $\mathbf{b} \mapsto \mathbf{a} \mapsto \check{\mathbf{x}}$ is non-degenerate (away from $\check{\mathbf{x}} = 0$) iff

$$\det \mathbf{a}_\mathbf{b} = -\ell_\varphi \neq 0 \quad \text{where} \quad \partial_\varphi = \partial_\phi - \partial_\beta \tag{20}$$

(∂_φ is the partial derivative that would result from a further change to coordinates (ϑ, φ) where $\varphi = \phi$ and $\vartheta = \theta$ (see Fig. 4). Note $\partial_\varphi \neq \partial_\phi$, because ∂_φ varies ϕ while holding θ fixed, whereas ∂_ϕ holds β fixed.) Then (combine $\check{\mathbf{x}} \times \partial \check{\mathbf{x}} = e^{2\ell} \partial \theta$, (12), (19) and (20))

$$\check{q}^\beta \stackrel{(15)}{=} \frac{-2\mu}{\partial_\beta \log \check{\psi}_\varphi} . \tag{21}$$

By the same arguments (17) reduces to

$$\check{\omega} = \Omega(\phi) \check{\psi}_\varphi^{-\frac{1}{2\mu}} . \tag{22}$$

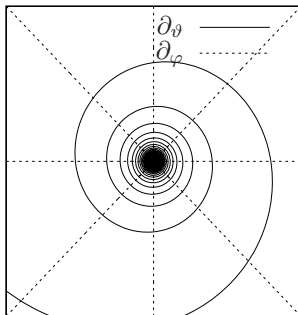


Figure 4: (ϑ, φ) coordinates. ∂_φ is a derivative in radial direction.

3 Background solution

The last remaining equation to be solved is the curl constraint $\Delta_{\check{\mathbf{x}}}\check{\psi} = \check{\omega}$, which transforms by a lengthy but elementary calculation (see [10, section 3.3]) to

$$0 = \underbrace{\partial_\varphi \left(2\check{\psi}_\beta \left(1 + \left(\frac{\check{\psi}_\beta \phi}{2\check{\psi}_\beta} \right)^2 \right) \frac{\check{\psi}_\varphi}{\check{\psi}_\beta \phi} - \frac{\check{\psi}_\phi \check{\psi}_\beta \phi}{2\check{\psi}_\beta} \right)}_{=:g^{(\varphi)}} + \underbrace{\partial_\phi \left(\frac{\check{\psi}_\beta \phi \cdot \check{\psi}_\phi - \check{\psi}_\beta \phi \cdot \check{\psi}_\varphi}{2\check{\psi}_\beta} \right)}_{=:g^{(\phi)}} + \underbrace{\frac{1}{2\mu} \check{\psi}_\beta \phi \check{\psi}_\varphi^{-\frac{1}{2\mu}} \Omega}_{=:g^{(0)}} \quad (23)$$

$\underbrace{\hspace{15em}}_{=: \check{F}}$

It is a 3rd order equation because the change of variables introduces into the outer divergence the matrix $\text{adj } \check{\mathbf{x}}_{\mathbf{b}}$ which yields, via $\check{r}^2 = -\check{\psi}_\beta / \mu$, second derivatives of $\check{\psi}$.

Although the equation looks intimidating, we can identify some particular solutions that are inherited from the \mathbf{x}, t form. An important class are the stationary radial ones: $\omega(t, \mathbf{x}) = \omega(r)$. Then \mathbf{v} is purely angular, hence orthogonal to $\nabla\omega$, so that the vorticity equation $0 = \mathbf{v} \cdot \nabla\omega$ is trivially satisfied. The initial condition (3) with $\check{\omega} = \check{\omega}_0 = \text{const}$ yields the special case

$$\omega = \check{\omega}_0 r^{-\frac{1}{\mu}} \quad , \quad \psi = \left(2 - \frac{1}{\mu} \right)^{-2} \check{\omega}_0 r^{2-\frac{1}{\mu}} \quad (24)$$

These solutions are not only stationary, but also self-similar in the sense (6):

$$\check{\omega} = \check{\omega}_0 \check{r}^{-\frac{1}{\mu}} \quad , \quad \check{\psi} = \left(2 - \frac{1}{\mu} \right)^{-2} \check{\omega}_0 \check{r}^{2-\frac{1}{\mu}} \quad (25)$$

(The solutions we obtain for $\check{\omega} \neq \text{const}$ are *not* stationary.)

Our particular solutions (25) are multiples of the *background solution*

$$\check{\psi}_0 = \frac{1}{2\mu - 1} \beta^{1-2\mu} \quad (26)$$

To see this, calculate

$$\check{r}^2 = e^{2\ell} \stackrel{(19)}{=} -\frac{1}{\mu} \partial_\beta \check{\psi}_0 = \mu \beta^{-2\mu} \Leftrightarrow \beta = (\mu^{-\frac{1}{2}} \check{r})^{-1/\mu}, \quad (27)$$

and substitute into (26) to obtain (25). $\check{\psi} = \check{\psi}_0$ solves (23) for

$$\Omega_0 = \frac{2\mu - 1}{\mu}. \quad (28)$$

To calculate the pseudo-streamlines of $\check{\psi}_0$ for each ϕ , substitute $\beta \stackrel{(18)}{=} \theta - \phi$ into (27):

$$\check{r} = \mu^{\frac{1}{2}} (\theta - \phi)^{-\mu}. \quad (29)$$

This is the \check{r} - θ -relationship for an algebraic spiral. $\check{r} \rightarrow \infty$ corresponds to $\theta \searrow \phi$, so ϕ is the angle of the pseudo-streamline at infinity.

4 Birkhoff-Rott spirals

Kaden ([12], see also [23]) previously obtained algebraic vortex spirals by a heuristic argument: consider the Birkhoff-Rott equation

$$\partial_t Z(t, \Gamma) = W^* = \left(\frac{1}{2\pi i} \text{p.v.} \int \frac{d\Gamma'}{Z(t, \Gamma) - Z(t, \Gamma')} \right)^* \quad (30)$$

(where $Z = x + iy$ parametrizes a curve on which vorticity is supported, with $W = v^x - iv^y$ the *complex velocity*) and seek self-similar solutions

$$z(t, \Gamma) = t^\mu \check{z}(\gamma) \quad , \quad \gamma = t^{1-2\mu} \Gamma \quad , \quad (31)$$

leading to

$$(1 - 2\mu)\gamma \check{Z}_\gamma + \mu \check{Z} = \check{W}^* = \left(\frac{1}{2\pi i} \text{p.v.} \int \frac{d\gamma'}{\check{Z}(\gamma) - \check{Z}(\gamma')} \right)^*. \quad (32)$$

Spirals observed in nature have almost circular spiral turns (as in Fig. 1 right), with near-uniform distribution of circulation γ . We may approximate each by an exact uniform vortex circle centered in the origin. Such circles induce $\check{W} = 0$ in their interior, but for $Z(\gamma)$ outside we may replace the circle by a point vortex of equal circulation in the origin without changing \check{W} . Accordingly, Kaden's

approximation is to replace the spiral half closer to the origin ($\gamma' < \gamma$) by such a point vortex and to neglect the other half:

$$(1 - 2\mu)\gamma \check{Z}_\gamma + \mu \check{Z} = \left(\frac{1}{2\pi i} \frac{1}{\check{Z}(\gamma)} \right)^* . \tag{33}$$

Substitute $z(\gamma) = \check{r}(\gamma)e^{i\theta(\gamma)}$, divide by $e^{i\theta}$ and separate real and imaginary part:

$$(1 - 2\mu)\gamma(\check{r}_\gamma + i\check{r}\theta_\gamma) + \mu\check{r} = \left(\frac{1}{2\pi i} \check{r}^{-1} \right)^* . \tag{34}$$

Solution:

$$\check{r}(\theta) = C\theta^{-\mu} \tag{35}$$

for some constant C .

We confirm Kaden’s heuristic argument, which produces algebraic spirals from an approximation, by constructing exact solutions of the Euler equations. Our argument is not meaningful for the background solution, since it does not have “stratified” vorticity so that pseudo-streamlines are merely mathematical imaginations, but once we perturb the background we have physically observable spirals.

5 Linearization

We seek nontrivial solutions by linearizing the equation around the background $\check{\psi} = \check{\psi}_0, \Omega = \Omega_0$: another lengthy but elementary calculation yields the Fréchet derivative

$$\frac{\partial \check{F}}{\partial \check{\psi}}[\check{\psi}_0, \Omega_0] = c_1 \beta^{c_2} \left(\underbrace{\left((\beta \partial_\phi)^2 + (\mu \partial_\phi)^2 \right) (\beta \partial_\beta + 2\mu)}_{=R} - \underbrace{(2\mu - 1)(\beta \partial_\phi + \beta \partial_\beta)}_{=E} \right) \tag{36}$$

(for some constants c_1, c_2). Take the Fourier-transform in ϕ (dual variable $n \in \mathbb{Z}$):

$$R = (\beta(in - \partial_\beta) + n\mu)(\beta(in - \partial_\beta) - n\mu)(\beta \partial_\beta + 2\mu) , \quad E = (2\mu - 1)\beta in . \tag{37}$$

We observe the essential fact that the linearization decomposes (after Fourier transform in ϕ) into infinitely many ordinary differential operators. Reason: we linearized around a function $\check{\psi}_0(\beta, \phi)$ that is constant in ϕ (see (26)), so that only β appears in the variable coefficients.

It is also convenient that R is fully factored into 1st order operators. We invert the linearized operator by first inverting R and then absorbing E as a perturbation.

To that end it is convenient to exploit $N \gg 1$: at $n = 0$ we have $E = 0$, we may ignore $0 < |n| < N$ by symmetry, and for $|n| \geq N \gg 1$ the operator R , which contains two n , dominates E (only the μn matter for “size”, not the in , as can be seen from integral kernels of the 1st order factor inverses).

6 Nonlinearity, iteration

Having inverted the linearization, the full problem is solved by iteration (see [11] for a detailed discussion of the difficult choice of correct function spaces).

A key difficulty of the nonlinear problem is the asymptotic behaviour as $\beta \rightarrow \infty$. To solve the problem for nonconstant perturbations $\hat{\omega}$ of the constant $\hat{\omega}_0$, we need to perturb the background solution $\check{\psi}$ and hence the coordinate transformation from β, ϕ to $\check{\mathbf{x}}$, whose constant- ϕ curves form algebraic spirals. A perturbation that does not decay sufficiently fast towards the spiral center will cause the curves to self-intersect (Fig. 5). This can easily happen since the spiral turns are very densely packed. Self-intersection corresponds to a degenerate coordinate transform $\mathbf{b} \mapsto \check{\mathbf{x}}$ which would manifest itself in the equations (23) as denominators and radicands reaching zero.

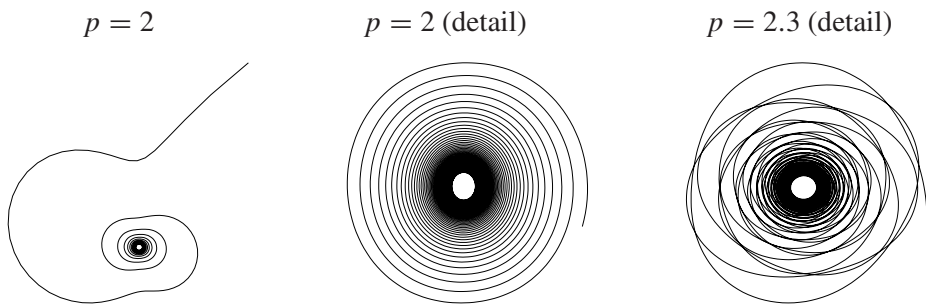


Figure 5: The spiral $\mathbb{R}_+ \ni \beta \mapsto \beta^{-1}e^{i\beta}$ perturbed to $\beta^{-1}e^{i\beta}(1 + \alpha\beta^{-\delta}e^{ip\beta})$, with $\alpha = 0.5$, $\delta = 0.7$. (The spiral center is not drawn, leaving a white spot in the middle.) Integer frequency p : the perturbation is barely noticeable near the center. Non-integer frequency p : physically unreasonable self-intersection.

Of the three derivatives $\partial_\phi = \partial_\phi - \partial_\beta$ and $\partial_\beta, \partial_\phi$ in (23), one may appear redundant, but our way of writing the equation actually makes a crucial choice: we are separating terms by β decay; a ∂_ϕ indicates an additional β^{-1} as compared to $\partial_\beta, \partial_\phi$. That is the key step in overcoming the decay problem.

Acknowledgments. This material is based upon work partially supported by the National Science Foundation under Grant No. NSF DMS-1054115 and by a Sloan Foundation Research Fellowship.

References

- [1] A. Bertozzi and P. Constantin. *Global regularity for vortex patches*. Commun. Math. Phys., **152** (1993), 19–28.
- [2] G. Ben-Dor. *Shock wave reflection phenomena*. Springer (1992).
- [3] J.-Y. Chemin. *Persistence de structures geometriques dans les fluides incompressibles bidimensionnels*. Ann. Ec. Norm. Supér., **26**(4) (1993), 1–16.
- [4] R. Danchin. *Evolution temporelle d'une poche de tourbillon singulière*. Commun. Partial. Diff. Eqns., **22** (1997), 685–721.
- [5] J.-M. Delort. *Existence de nappes de tourbillon en dimension deux*. J. Amer. Math. Soc., **4**(3) (1991), 553–586.
- [6] R. DiPerna and A. Majda. *Oscillations and concentrations in weak solutions of the incompressible euler equations*. Commun. Math. Phys., **108** (1987), 667–689.
- [7] V. Elling. *A possible counterexample to well-posedness of entropy solutions and to Godunov scheme convergence*. Math. Comp., **75** (2006), 1721–1733.
- [8] V. Elling. *The carbuncle phenomenon is incurable*. Acta Math. Sci. (ser. B), **29**(6) (2009), 1647–1656.
- [9] V. Elling. *Existence of algebraic vortex spirals*. Hyperbolic problems. Theory, Numerics and Applications., Ser. Contemp. Appl. Math. CAM, 17, vol. 1, World Sci. Publishing, Singapore, (2012), 203–214.
- [10] V. Elling. *Algebraic spiral solutions of 2d incompressible euler*. J. Diff. Eqns., **255**(11) (2013), 3749–3787.
- [11] V. Elling. *Self-similar 2d euler solutions with mixed-sign vorticity*, (submitted), (2014).
- [12] H. Kaden. *Aufwicklung einer unstablen Unstetigkeitsfläche*. Ingenieur-Archiv, **2** (1931), 140–168.
- [13] R. Krasny. *Computing vortex sheet motion*. Proceedings of the International Congress of Mathematicians, **I,II** (1991), 1573–1583.
- [14] M.C. Lopes-Filho, J. Lowengrub, H.J. Nussenzweig Lopes and Yuxi Zheng. *Numerical evidence of nonuniqueness in the evolution of vortex sheets*. ESAIM:M2AN, **40** (2006), 225–237.
- [15] P.-L. Lions. *Mathematical topics in fluid mechanics*. Oxford University Press, (1996).
- [16] C. De Lellis and L. Székelyhidi Jr. *The Euler equations as a differential inclusion*. Ann. Math., **170**(3) (2009), 1417–1436.

- [17] C. De Lellis and L. Székelyhidi Jr. *On admissibility criteria for weak solutions of the Euler equations*. Arch. Rat. Mech. Anal., **195**(1) (2010), 225–260.
- [18] A. Majda and A. Bertozzi. *Vorticity and incompressible flow*. Cambridge University Press (2002).
- [19] D.W. Moore. *The rolling-up of a semi-infinite vortex sheet*. Proc. Roy. Soc. London A, **345** (1975), 417–430.
- [20] M. Nitsche, M.A. Taylor and R. Krasny. *Comparison of regularizations of vortex sheet motion*. Comp. Fluid Solid Mech. (2003).
- [21] D. Pullin. *The large-scale structure of unsteady self-similar rolled-up vortex sheets*. J. Fluid Mech., **88**(3) (1978), 401–430.
- [22] D. Pullin. *On similarity flows containing two-branched vortex sheets*. Mathematical aspect of vortex dynamics (R. Caflisch, ed.), SIAM, (1989), 97–106.
- [23] N. Rott. *Diffraction of a weak shock with vortex generation*. J. Fluid Mech., **1** (1956), 111–128.
- [24] P.G. Saffman. *Vortex dynamics*, Cambridge University Press (1992).
- [25] V. Scheffer. *An inviscid flow with compact support in space-time*. J. Geom. Anal., **3** (1993), 343–401.
- [26] A. Shnirelman. *On the nonuniqueness of weak solutions of the Euler equation*. Comm. Pure Appl. Math., **50** (1997), 1261–1286.
- [27] A. Shnirelman. *Weak solutions with decreasing energy of the incompressible Euler equations*. Comm. Math. Phys., **210** (2000), 541–603.
- [28] M. van Dyke. *An album of fluid motion*. The Parabolic Press, Stanford, California (1982).
- [29] M. Vishik. *Incompressible flows of an ideal fluid with vorticity in borderline spaces of Besov type*. Ann. Sci École Norm. Sup. (4), **32** (1999), 769–812.
- [30] V. Yudovich. *Non-stationary flow of an ideal incompressible liquid*. Comp. Math. Math. Phys., **3** (1963), 1407–1457.
- [31] V.I. Yudovich. *Uniqueness theorem for the basic nonstationary problem in the dynamics of an ideal incompressible fluid*. Math. Res. Lett., **2** (1995), 27–38.

Volker Elling

University of Michigan
Department of Mathematics
530 Church St
Ann Arbor, MI 48109
USA

E-mail: velling@umich.edu